Biochimica et Biophysica Acta 1788 (2009) 1263–1270

Contents lists available at ScienceDirect

Biochimica et Biophysica Acta

journal homepage: www.elsevier.com/locate/bbamem

IR spectroscopy as a new tool for evidencing antitumor drug signatures

Régis Gasper [a], Janique Dewelle [b], Robert Kiss [c], Tatjana Mijatovic [b], Erik Goormaghtigh [a,*]

[a] Laboratory for the Structure and Function of Biological Membranes, Center for Structural Biology and Bioinformatics, Université Libre de Bruxelles (ULB), Brussels, Belgium
[b] Unibioscreen SA, Brussels, Belgium
[c] Laboratory of Toxicology, Institute of Pharmacy, Université Libre de Bruxelles (ULB), Brussels, Belgium

ARTICLE INFO

Article history:
Received 17 November 2008
Received in revised form 12 January 2009
Accepted 18 February 2009
Available online 27 February 2009

Keywords:
IR spectroscopy
Ouabain
Cancer
Sodium pump

ABSTRACT

There is a growing interest for screening antitumor drugs for their mechanism of action on cancer cells. Yet, screening for "modes of action" presents a technical challenge that is beyond the capability of conventional methods used in cellular or molecular biology. Several studies have highlighted the advantages of using infrared spectroscopy for diagnostic purposes at the clinical level for identifying cell types. In the present work, we suggest that the Fourier Transform Infrared (FTIR) spectrum of cells exposed to anti-cancer drugs could offer a unique opportunity to obtain a fingerprint of all molecules present in the cells and to observe, with a high sensitivity, the metabolic changes induced by potential anti-cancer drugs. Ouabain is one of the most potent cardenolides, which acts by inhibiting sodium pump activity. Cardenolides represent a class of compounds that are intended to soon enter clinical trials in oncology. In order to evaluate the potential of infrared spectroscopy to yield a signature for ouabain action on cancer cells, human prostate cancer PC-3 cells were treated with 36 nM ouabain, a sub-lethal concentration. Using ouabain as a model, we have thus demonstrated the possibility of using IR spectroscopy in the assessment of the global effects of an investigational compound on the cell constituents, thus contributing to setting up a new method for screening for novel anti-cancer agents in general, and potential anti-cancer cardenolides in particular. The most spectacular data obtained strongly suggest a modification in the nature of the cell lipids.

1. Introduction

The number of anti-cancer agents that fail in the clinic far outweighs those considered effective, suggesting that the selection procedure for progression of drug molecules into the clinic requires improvement [1]. Traditionally, new drugs are evaluated for their potential to kill cancer cell lines. This approach is obviously not sufficient, and molecules with new modes of action are required. In turn, there is a tremendous interest in obtaining a fingerprint of their mechanism of action on the cells.

Screening for "modes of action" presents a technical challenge that is beyond the practical capability of conventional methods used in cellular or molecular biology. The infrared spectrum of cells exposed to anti-cancer drugs could offer an opportunity to obtain a fingerprint of all molecules present in the cells and, with a high sensitivity observe the metabolic changes induced by the drugs. IR spectroscopy is based on the absorption of infrared light by vibrational transitions in covalent bonds. While the intensities provide quantitative information, the frequencies relate to the nature of these bonds, their structure, and their molecular environment. In complex systems such as cells, an infrared spectrum is the sum of the contributions gathered from the proteins, the lipids, the nucleic acids, and all other chemical species present in the cells. The spectra could thus be used as signatures to provide evidence of global effects of a compound on all of the cell constituents.

In the eighties, it was demonstrated that the FTIR spectrum of bacteria provides a unique fingerprint that allows the identification of bacteria species [2,3]. Hundreds of applications have been published since this pioneering work. In the nineties, it was shown that tumor cells can be distinguished from their normal counterparts by observation of their FTIR spectra [4,5]. Later, with advances in instrumentation and in multivariate statistics, tumor cell lines with different biological behaviour could be separated. For instance, the aggressiveness of different glioma cell lines was successfully predicted from their FTIR spectra while no molecular biology means were available for this purpose [6]. Similarly, the distinction of premalignant from malignant cells also became available using specific parameters obtained from Fourier Transform Infrared spectra, making it a rapid and reagent-free method [7].

We now suggest that cells treated with potentially useful drugs will experience metabolic modifications correlated with their cellular mode of action. Because the infrared spectrum of cells yields a precise

Abbreviations: IR, infrared; FTIR, Fourier Transform infrared; CS, cardiotonic steroid; PCA, principal component analysis; PS, phosphatidylserine; GGR, global growth ratio; CCD, charge coupled device

* Corresponding author. Center for Structural Biology and Bioinformatics, Laboratory for the Structure and Function of Biological Membranes, Campus Plaine CP206/02, Université Libre de Bruxelles, Bld du Triomphe 2, CP206/2, B1050 Brussels, Belgium. Tel.: +32 2 650 53 86; fax: +32 2 650 53 82.
E-mail address: egoor@ulb.ac.be (E. Goormaghtigh).

0005-2736/$ – see front matter © 2009 Elsevier B.V. All rights reserved.
doi:10.1016/j.bbamem.2009.02.016

image of all the chemical bonds present in the sample, different drug actions are likely to each yield a unique fingerprint characteristic of the "mode of action" of the therapeutical agent under investigation. In turn, drug-induced metabolic disorders should be amenable to classification similar to the ways in which bacteria gender, species, and strains can be classified.

In the present paper, we examine the feasibility of the approach by investigating the subtle differences that occur in a human prostate cancer cell line (the PC-3 model) upon exposure to sub-lethal concentrations of ouabain, a well-known cardiotonic steroid [8]. Cardiotonic steroids, or cardiotonic glycosides, represent a group of compounds that share the capacity to bind to the extra-cellular surface of the main ion transport protein in the cell, the membrane-embedded sodium pump (Na^+/K^+-ATPase), and have been widely used for the treatment of heart failure. Early epidemiological evaluations and subsequent demonstration of anti-cancer activity in vitro and in vivo have indicated the possibility of developing this class of compound as chemotherapeutic agents in oncology [8]. The sodium pump, the receptor of cardiotonic steroid, might be an important target for the development of anti-cancer drugs because it serves as a versatile signal transducer. It is a key player in cell adhesion, and its aberrant expression and activity are implicated in the development and progression of different cancers. In addition to transporting ions, the sodium pump interacts with neighbouring membrane proteins (thus forming a "sodium pump signalosome") and precipitates cytosolic cascades of signaling proteins used to send messages to the intra-cellular organelles [8]. Ouabain is used here to demonstrate the feasibility of the approach and to illustrate the wealth of information present in the FTIR spectra. We show that FTIR detects subtle metabolic modifications and sheds some light on the chemical modifications induced upon ouabain exposure.

2. Materials and methods

2.1. Compounds

Ouabain was purchased from Acros Organics (Geel, Belgium). Lipids were obtained from Avanti (Alabaster, USA).

2.2. Cell culture

The human prostate cancer PC-3 (CRL-1435) cell line was obtained from the American Type Culture Collection (ATCC, Manassas, VA) and was maintained according to the supplier's instructions. The cells were incubated at 37 °C in sealed (airtight) Falcon plastic dishes (Nunc, Invitrogen SA, Merelbeke, Belgium) in a humidified atmosphere of 5% CO_2. The cells were kept in exponential growth in RPMI medium supplemented with 10% fetal bovine serum (FBS), 1% penicillin/streptomycin (an antibiotic/antimycotic solution), and 1% kanamycin to prevent mycoplasms. Medium and FBS were purchased from Gibco, Invitrogen, Merelbeke, Belgium. Penicillin/strepromycin and kanamycin solutions came from Sigma-Aldrich SA, Bornem, Belgium.

For FTIR spectroscopy, cells were suspended by means of a five-minute treatment with trypsin/EDTA buffer (Gibco, Invitrogen SA, Merelbeke, Belgium). The reaction was stopped by adding 1 ml of culture medium. The cells were pelleted by a 2-minute centrifugation (200 rpm), and washed three times in isotonic solution (NaCl, 0.9%) to ensure complete removal of trypsin and culture medium. They were then suspended in 30 µl of the NaCl solution.

2.3. In vitro overall growth determination

Overall cell growth was assessed by means of the colorimetric MTT (3-[4,5-dimethylthiazol-2yl]-diphenyltetrazolium bromide, Sigma, Bornem, Belgium) assay, as detailed elsewhere [9,10]. The cells were incubated for 72 h in the presence or the absence (controls) of the tested compounds. Drug concentrations ranged between 10^{-9} and 10^{-5} M (with semi-log concentration increases). Experiments were carried out in sextuplicate.

2.4. Quantitative videomicroscopy for cellular imaging

Human PC-3 prostate cancer cell migration and proliferation with and without treatments were characterized in vitro by quantitative videomicroscopy, as previously described [6,11].

PC-3 cells were grown to confluence in Petri dishes (35 mm diameter NUNC, VWR Int., Leuven, Belgium). Scratch wounds were made by creating a linear denuded region using a pipette tip. The cells were washed twice with PBS prior being cultured in the absence (controls) or presence of 36 nM ouabain. Computer-assisted phase-contrast microscopy was used to record a digital image of the denuded region every 10 min over 72 h. Each experimental condition was tested in triplicate.

2.5. FTIR spectroscopy

All measurements were carried out on a Bruker Equinox 55 FT-IR spectrometer (Bruker, Karlsruhe, Germany) equipped with a liquid N_2-refrigerated mercury cadmium Telluride detector. All spectra were recorded by attenuated total reflection (for a review, see [12]). A diamond internal reflection element was used on a Golden Gate Micro-ATR from Specac (Orpington, UK). The angle of incidence was 45°. A 0.5 µl amount of the cell re-suspended in about twice the volume of the pellet (2 min, 300 *g*) was deposited on the diamond crystal (about 3×10^4 cells per smear). The sample was quickly evaporated in N_2 flux to obtain a homogenous film of whole cells, as ascertained by microscope examination. The FTIR measurements were recorded between 4000 and 800 cm^{-1}. Each spectrum was obtained by averaging 256 scans recorded at a resolution of 2 cm^{-1}. Three independent cultures were grown for each condition and three samples were taken from each culture for infrared measurement, thus generating a total of nine spectra per condition, as previously described [6].

2.6. Lipid extraction

Total lipid extraction from PC-3 cells was obtained according to the protocol of Bligh and Dyer [13]. Briefly, three steps were carried out: (i) addition of 125 µl of chloroform/250 µl of methanol to 100 µl of sample and vortex of the resulting solution, (ii) addition of 8.4 µl of hydrochloric acid (6 M) and 125 µl of chloroform and vortex of the solution, (iii) addition of 125 µl of pure desalted water, vortex of the solution again, and centrifuging for 10 min at 300 *g*. Total lipid content was collected in the lower phase.

2.7. Data analysis

The FTIR data were preprocessed as follows. First, the water vapor contribution was subtracted, and then the spectra were baseline-corrected and normalized for equal area between 2995–2800 and 1765–950 cm^{-1}. The spectra were finally smoothed at a final resolution of 4 cm^{-1} by apodization of their Fourier transform by a Gaussian line.

In IR spectra, each wavelength is a variable, i.e., about 1000 wavelengths are associated with biological molecule absorptions. With at least nine spectra for each condition, the number of variables submitted to statistical analysis quickly becomes extremely large. Data are best handled after Principal Component Analysis (PCA), which is an unsupervised statistical method that enables a reduction of variables by building linear combinations of wavenumbers that vary together. The first principal component (PC) accounts for most of the variance present in the data set; the second is built with the residual

variance and is uncorrelated to the first one. The subsequent components are constructed the same way and account for progressively less variance. In practice, almost all the variance of the original data can be explained with three or four uncorrelated variables, reducing the description of each spectrum to three or four numbers representing the weight of the PCs. Simultaneously, these weights allow the unsupervised classification of the spectra. Such an observation does not suppose any *a priori* conditions on these groups. In the analyses reported here, the collection of spectra was mean-centered (the mean was removed from the individual spectra).

The different analyses were carried out by means of specific software generated in our lab (Matlab, Mathworks Inc).

3. Results

3.1. Ouabain-induced effects on the growth of human prostate cancer PC-3 cells

The use of cardiotonic steroids has been reported previously, many times as a means of potentially combating human refractory prostate cancer (for review see [8]), which is the reason why we chose to use human prostate PC-3 cancer cells as a study model. Among different cardiotonic steroids, ouabain (for structure see Fig. 1A) is one the most used both in physiology-related and anti-cancer pharmacological and toxicological assays. Cellular imaging is a video-microscopy technique enabling cell observation in time, which allows the evaluation of the effect of a given product on the morphology, motility, death, and proliferation of cells [14]. The cells are maintained in closed flasks containing buffered medium at a controlled temperature of 37 +/− 0.1 °C during the time required for the experiment (in this case 72 and 144 h). They are monitored by means of a phase-contrast microscope coupled with a CCD camera. A control monitor placed between the camera and the computer allows visualization at all times of what is occurring with the cells. A picture is taken every four minutes. Movies are made by compressing all pictures (Supplemental files) [11,14]. On basis of the pictures, the parameter "Global Growth Ratio" (GGR) is calculated. The GGR is the ratio between the number of cells on the last picture to that on the first picture in an experimental group. The GGR(T)/GGR(CT) is the ratio between the GGR in the treated group (T) over that in the control group (CT). Lower ratios indicate a decrease in proliferation of treated cells. Using the Global Growth Ratio, we were able to evidence a high anti-proliferative effect of ouabain on human prostate cancer PC-3 cells (Fig. 1B), when used at its IC_{50} of 36 nM. The IC_{50} was defined as the concentration that reduced the global growth of the cancer cells by 50% after three days culturing in the presence of the compounds, as assessed by MTT assay (data not shown). Furthermore, using computer-assisted videomicroscopy for cellular imaging (Fig. 1C), we were able to visualize the morphological changes and anti-proliferative effects induced by ouabain and to rule out the hypothesis of ouabain-triggered cell death resulting from induction of osmotic shock, apoptosis, senescence, or mitotic catastrophe when the compound is used at its IC_{50} concentration. Scratch-wound assays (Fig. 1D) were able to further confirm the

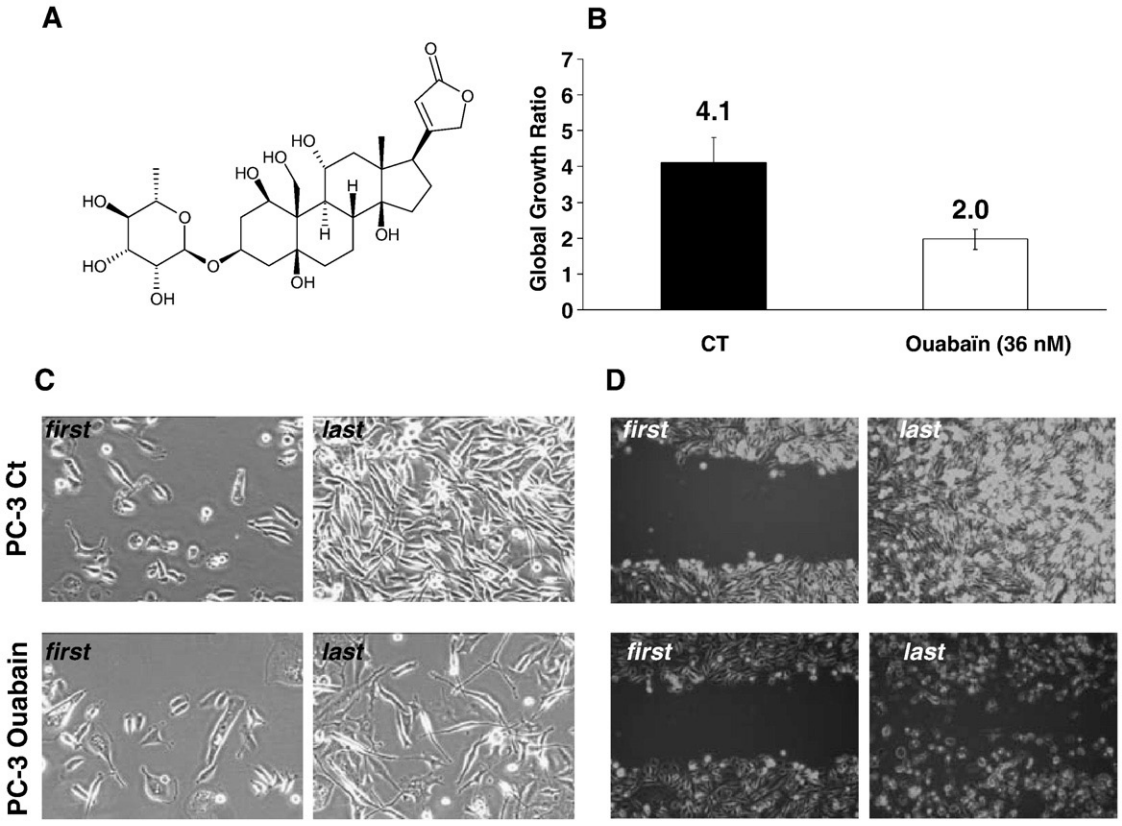

Fig. 1. Ouabain-mediated in vitro cytotoxic activity. (A) Chemical structure of ouabain. (B) Global Growth Ratio (GGR). On the basis of pictures obtained by cellular imaging, the parameter GGR is calculated. The GGR is the ratio between the number of cells on the last picture over that on the first picture in an experimental group. The GGR(T)/GGR(CT) is the ratio between the GGR in the treated group (T) over that in the control group (CT). Lower ratios indicate a decrease in proliferation of treated cells. (C) Computer-assisted video-microscopy analysis of PC-3 cells left untreated (control, upper panel) and 36 nM ouabain treated over 72 h (lower panel). Still images are presented at 0 min ("first") and 72 h ("last") selections of recordings. Movies are supplied as Supplementary data. Movies of (D) Scratch-wound assay made with PC-3 cells left untreated (control, upper panel) and 36 nM ouabain treated over 72 h (upper panel). Still images are presented at 0 min ("first") and 72 h ("last") selections of recordings. Movies are supplied as Supplementary data. A double click will activate the videos (recordings over the three day observation period have been speeded up to about one min). To minimize the file size of the generated video clips, they have been compressed using the DivX codec. The codec and a movie player are available at http://divx.com.

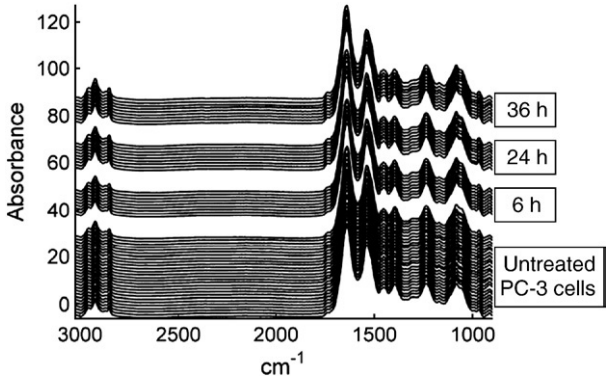

Fig. 2. FTIR spectra of PC3 cells grown in four experimental conditions. PC-3 cells were grown in the absence or in the presence of 36 nM ouabain for 6, 24, and 36 h. For each experimental condition, three samples were collected from three independent cell cultures, yielding a total of nine samples per condition. The spectra of four experimental conditions are displayed with successive slight shifts to the top for better readability.

ouabain-mediated cytotoxic effect on PC-3 cells. In this paper, the first and the last images of recordings are presented, while the movies can be visualized in the Supplementary information. Indeed, the still images presented in Fig. 1C clearly evidence the anti-proliferative effect of ouabain on human prostate PC-3 cancer cells (see the difference in cell number and morphology on the "last" pictures on untreated and ouabain-treated cells). Furthermore, while untreated cells are able to completely fill the wounded region (Fig. 1D), the ouabain-treated cells are unable to fill the wounded region and died before the end of observation time.

3.2. Evaluation of the potential of infrared spectroscopy to yield a signature for ouabain action on cells

In order to evaluate the potential of infrared spectroscopy to yield a signature for ouabain action on cells, PC-3 cells were grown in the absence or in the presence of 36 nM ouabain for 6, 24, and 36 h. For each experimental condition, three independent cell cultures were grown over a period of one year. From each cell culture, three samples were tested yielding a total of nine samples for each condition along with the corresponding controls (called the "zero" time). Importantly, the analyses described below did not show any significant difference between the spectra of untreated cells recorded at different periods of the year nor at different growth times. It has been shown that cells harvested in either the exponential growing stage or the plateau phase exhibit different cells spectra [15]. Despite this, in the present work, cells were always collected in exponential phase, and we also checked for spectral variability due to the growth stages. The data obtained (not shown) gave evidence for insignificant differences with respect to spectral differences highlighted after drug incubation. In turn, we can assume that the observed spectral modifications observed in the presence of ouabain are strictly related to ouabain-induced metabolic changes on PC-3 cells. Trypan blue was used to check the viability of the cells. For each condition, the viability rate was above 95% (data not shown), demonstrating that the FTIR measurements were not performed on dying cells. Fig. 2 shows the spectra obtained under four experimental conditions. These spectra are very similar at first glance, and can be roughly divided into three main regions:

1) Between 3000 cm^{-1} and 2800 cm^{-1}, the absorption is dominated by the stretching vibration of the CH_2 and CH_3 groups contained mainly in the lipid acyl chains and to a much lesser extent by the proteins of the cells.
2) Between 1800 cm^{-1} and 1300 cm^{-1}, the absorptions are primarily due to the proteins, with some absorptions from the lipids. The shoulder present at 1738 cm^{-1} is assigned to the ester C=O stretching of the phospholipids [16,17] and is not overlapped by contributions from DNA and proteins. The stretching of the protein amide C=O bonds takes place at 1650 cm^{-1} (named Amide I). This band is sensitive to the secondary structure of proteins [12]. The deformation of the protein amide N–H bond (Amide II) appears at 1540 cm^{-1}. The bands between 1480 and 1300 cm^{-1} are caused by the amino acid side chains and fatty acids.
3) Between 1300 cm^{-1} and 900 cm^{-1}, the absorptions result from carbohydrates as well as from phosphates mainly associated with nucleic acids, i.e., DNA and RNA. The absorption bands at 1241 cm^{-1} and 1085 cm^{-1} [18] are characteristic of the asymmetric and symmetric phosphodiester vibration of nucleic acids. Various glycogen vibrations are superimposed between 1150 and 1025 cm^{-1} [17,19]. The small peak appearing at 968 cm^{-1} is assigned to C–O phosphodiester moieties.

The region between 2800 and 1800 cm^{-1} has no absorption bands from the cells, but contains the contribution of atmospheric CO_2 (2350 cm^{-1}).

3.3. PCA spectral analysis

A PCA (Principal Component Analysis) analysis was first carried out as an unsupervised test potentially able to classify the data. The result of a PCA analysis is presented in Fig. 3 as the projection of the cell spectra at different ouabain incubation time points on the first two principal components. The percentage between brackets represents the fraction of the total variance described by the principal component. More than 86% of the spectral variance was thus explained by the data reported in Fig. 3. It appears clearly from Fig. 3 that PCA allowed the separation between the controls, 6-hour incubation, and (together) 24 and 36-hour incubation times. Projection on the fourth principal component (not shown, 6% of the total variance) allowed the separation between the 24 and 36 h cell treatments with 36 nM ouabain. Even though unsupervised, PCA analysis indicated that the effect of ouabain on PC-3 cells can be evidenced through the fingerprint provided by their FTIR spectra. Furthermore, the time dependence of the effects also appeared from the analysis.

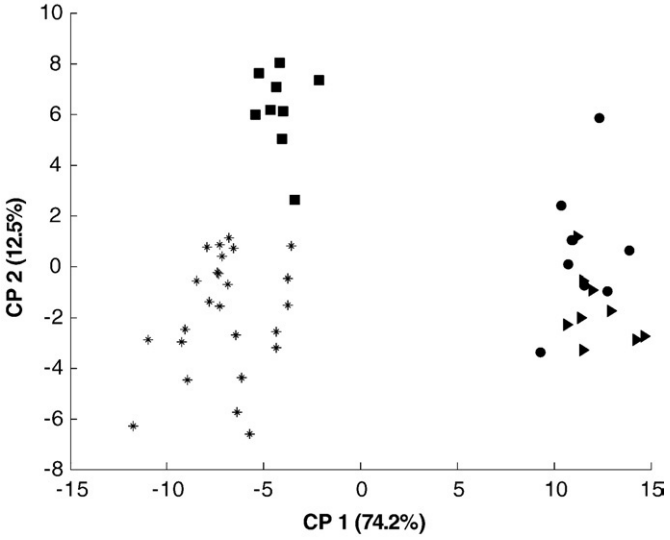

Fig. 3. PCA analysis of the FTIR spectra of cells grown in four experimental conditions. Each point of the plot is the projection of a spectrum in the principal components PC1–PC2 space. Black stars represent the spectra from untreated cells. The other symbols are used for the different incubation time points: ■ = 6 h, ● = 24 h, ▶ = 36 h. The percentages between brackets represent the proportion of variance held in the principal components.

3.4. Student t-tests

To gain more insight into the chemical modifications induced at the different stages of the incubation, a Student *t*-test was performed between successive pairs of conditions. After computation of the mean spectra for each incubation condition, the differences between mean pairs were reported in Fig. 4, resulting in three curves: one for the early changes (6 h–0 h), one for the metabolic modifications induced by the drug after about one generation (24 h–6 h), and one for later changes (36 h–24 h). The positive and negative peaks in the difference spectra shown in Fig. 4 are representative of the molecules that are relatively more abundant (positive bands) or less abundant (negative bands) in the cells after treatment. Note that all the difference spectra presented in Fig. 4 are plotted on the same scale. Intensity of the peaks can thus be compared. Before computing the Student *t*-value, normality of the distribution of the absorbances at every wavenumber was checked by a Kolmogorov–Smirnov test on each subgroup. No significant deviation from a normal distribution could be detected for all treatment conditions. The Student test was performed with $\alpha = 0.01$ and a Bonferroni correction that divided α by the number of wavenumbers tested. In turn, the effective α value for each wavenumber was close to 3×10^{-6}. With this stringent criterion, every wavenumber was tested and a star was placed on the line when the Student test was positive (rejection of the equality of the means). Results are reported in Fig. 4. It can be observed that the Student positive wavenumbers appear as well-localized regions. This feature is easily explained when considering that adjacent wavenumbers are intrinsically correlated over the width of absorption bands.

After 6 h incubation, a limited number of regions were affected, mainly in the protein (around 1650 cm^{-1}) and the fingerprint regions between 1500 and 1200 cm^{-1}. Between 6 h and 24 h, large new significant differences appeared. The most spectacular ones are related to lipids, between 3000 and 2800 cm^{-1} ($\nu_{as}(CH_2)$ at 2922 cm^{-1}, $\nu_s(CH_2)$ at 2852 cm^{-1}, $\nu_{as}(CH_3)$ at 2955 cm^{-1}, $\nu_s(CH_3)$ at 2872 cm^{-1}), 1738 cm^{-1} (ν(C=O)), and 1465 cm^{-1} ($\delta_{as}(CH_2)$) [20]. The second most intense feature resulted from a shift in the Amide I region of the spectrum, which could indicate that, overall, the protein structure was affected. The third difference spectrum, 36 minus 24 h, did not reveal any further large modification of the situation found after 24 h incubation, except a notable change at the level of the lipid double bound at 3005 cm^{-1} (ν(CH) on unsaturated carbon) [20]. The data reported above strongly suggest that FTIR spectroscopy is not only able to sense cellular modifications induced by ouabain, but also to qualitatively follow the progression of these changes during the course of treatment.

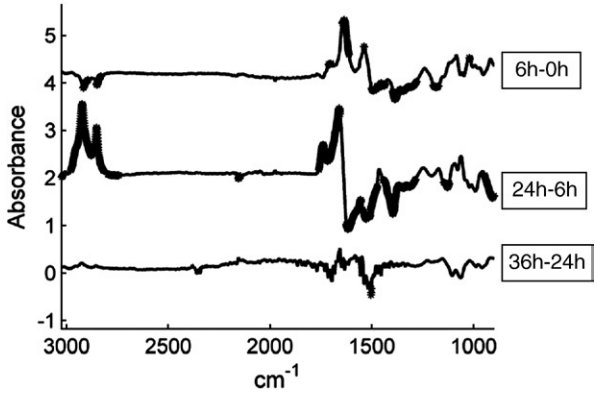

Fig. 4. Differences between mean spectra for pairs of conditions for entire cells. Each spectrum is the difference between two average spectra from pairs of experimental conditions. A Student *t*-test was computed for every wavenumber with a significance level of $\alpha = 0.01$ and a Bonferroni correction. Each marked wavenumber (highlighted area) represents a statistically significant difference between the means.

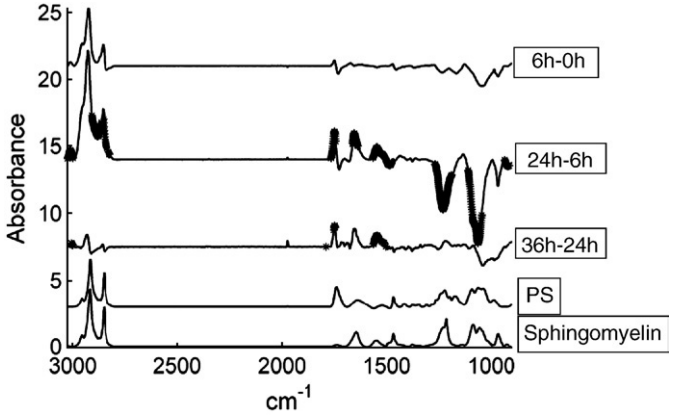

Fig. 5. Differences between mean spectra for pairs of conditions for lipid extracts. For Fig. 4, each spectrum is the difference between two average spectra of lipid extracts from PC-3 cells grown in four experimental conditions. A Student *t*-test was computed for every wavenumber with a significance level of $\alpha = 0.01$ and a Bonferroni correction. Each marked wavenumber (highlighted area) represents a statistically significant difference between the means. The spectra from pure phosphatidylserine and pure sphingomyelin are also reported.

The appearance of a strong lipid contribution in the Student analysis after 24 h (but not after 6 h) indicates that either the lipid content in the cell varied or the nature of the lipid varied. In order to test this hypothesis we performed a total lipid extract from cells collected after different ouabain incubation times.

3.5. Ouabain treatment of PC-3 cells affects lipid content and/or lipid type

The Student tests suggested that the lipid content was strongly affected by ouabain treatment. To gain more insight into the molecules involved, we analyzed lipid extracts obtained from PC-3 cells grown in the same conditions and similarly incubated with ouabain for 6, 24, and 36 h. FTIR spectra of entire cells were recorded before lipid extraction in order to properly compare the cells and their lipid extract. The spectra of the cells were shown to be undistinguishable from the others recorded in the course of the present study (e.g., Fig. 2). The differences between pairs of mean spectra obtained in different conditions were also computed and the significance of the difference at every wavenumber was evaluated by a Student test (Fig. 4). As before, the positive/negative peaks that appear in the difference spectra (Fig. 5) arise from the chemical groups present in relatively higher/lower concentration after ouabain treatment. No significant difference was found after 6 h incubation in the presence of ouabain, in agreement with the previous results. Most of the differences appeared between 6 and 24 h, notably in the regions of $\nu_s(CH_2)$ at 2852 cm^{-1}, $\nu_s(CH_3)$ at 2872 cm^{-1}, ν(C=O) at 1738 cm^{-1} and ν(CH) on unsaturated carbon at 3005 cm^{-1} [20]. In addition, the phosphate bands $\nu(PO_2^-)$ at 1240 and 1085 cm^{-1} [20] were also significantly marked by the Student test. Between 24 and 36 h, fewer additional differences showed up, but as for the entire cells, the unsaturation of the acyl chains was further increased. Furthermore, the band located near 1550 cm^{-1}, already present after 24 h, continued its rise. To find out which lipids were implicated in the difference observed in 1700–1500 cm^{-1} region, we compared them to spectra of pure typical lipids from each subclass of eukaryote cell membrane (spectra not shown). Among the major phospholipids, bands in this spectral region were only present in sphingolipids and phosphatidylserine, but not in phosphatidylcholine, phosphatidylglycerol, phosphatidic acid, or cardiolipin. The bands between 1663 and 1635 cm^{-1} and between 1565 and 1475 cm^{-1} are typical of phosphatidylserine or sphingomyelin.

4. Discussion

Monitoring the overall changes occurring in the cell upon exposure to a drug is a complex task. So far, either specific markers have been used as indices of the changes or DNA microarrays have provided a global overview of protein synthesis activity. As seen from our result, infrared spectroscopy can also be a powerful tool for the study of biological systems. This technique records a fingerprint of all the molecules present in the cells, lipids, sugars, proteins, nucleic acids, etc. It senses not only the chemical nature of these molecules but also their conformations. It is very sensitive to protein conformation [21,22] and plays an important role in the determination of conformational illnesses [23,24]. Overall, the approach is very sensitive to any metabolic perturbations. This approach has already been used in several fields, such as classification of bacterial subspecies [3,25], differentiation of tumor and normal cells [26–29], and tumor cell behavior [6]. Because of the very high signal-to-noise ratio of FTIR spectra, metabolism perturbation induced by any drug should be distinguishable. In the work presented here, we tried to bring to light the metabolic modifications of PC-3 cells brought on by ouabain, one of the most studied cardenolides. Experimental conditions were selected (such as a decrease in the growth rate of the PC3 cells) and results were clearly established as assessed by camera imaging and scratch wound assays, while cell death was insignificant, as demonstrated by the trypan blue assay.

PCA analysis suggested that subtle differences in cell metabolism could be evidenced, including those occurring in the shortest incubation time in the presence of ouabain (6 h). A more chemically oriented view of the differences induced by ouabain treatment was provided by the difference spectra. The differences observed after 6 hour incubation (Fig. 4) were of small amplitude and not significant with the very stringent statistical test ($\alpha \sim 10^{-6}$), while observation of the PCA results (Fig. 3) demonstrated a clear separation from the untreated control cells. Between the 6 and 24 h time points, a progression of the previous effect was observed. Nevertheless, some new spectral areas appeared to be significantly modified upon ouabain treatment, including the entire C–H region between 3025 and 2800, the lipid ester carbonyl band around 1740 cm^{-1}, and the protein Amide I and II regions.

Quantitatively, the analysis of entire cells demonstrated that the area under the curve between 3000 and 2800 cm^{-1} was increased by 20% after 24 h of ouabain treatment. Because the absorption of the IR beam in this region is dominated by the contribution of the hydrocarbon chains of the lipids [16], a relative increase in the amount of lipids with respect to the other cell components after one day of ouabain treatment could be suggested. This conclusion was further supported by the concomitant increase of the lipid carbonyl group around 1740 cm^{-1}. Furthermore, the overall protein structure of PC-3 cells appeared to be significantly affected after 24 h of ouabain treatment. The positive peak around 1653 cm^{-1} arises from the α helix conformation of proteins and the negative contribution around 1636 cm^{-1} comes from the β sheet conformation [18,21,22,30–32]. In turn, the spectral features present in the difference spectra could be explained by a higher proportion of α helix and a lower proportion of β sheet after one day of ouabain treatment. Remarkably, after 36 h of incubation, no further change occurred except for a small region around 1500 cm^{-1} potentially assigned to lateral chains of protein amino acids.

Because of the clues revealed in the entire cell difference spectra, we carried out a similar analysis for lipid extracts obtained from PC-3 cells. After 6 h of treatment, the lipids were not affected by the action of ouabain (Fig. 5). This result demonstrates that the ouabain molecule itself cannot be responsible for the changes observed for longer incubation times. Most of the differences appeared after 24 h. The two negative peaks at 1241 and 1085 cm^{-1} were assigned $\nu_{as}(PO_2^-)$ and $\nu_s(PO_2^-)$ from the phospholipids [16]. These phosphate peaks appeared to be significantly affected by ouabain treatment for the lipid extracts but not for entire cells. This can be simply explained by the large amount of phosphate contributions from nucleic acid superimposing their contributions on entire cells, resulting in an increased variability of the FTIR data. The ratios between the areas of a number of IR absorption bands associated with the amount of CH_3, CH_2, C–H on unsaturated C=C bands, C=O, PO_2^-, and N–H (amine or amide) shed some light on molecular modifications occurring in the lipid extract. These ratios are reported in Table 1. The evolution in the lengths of the hydrocarbon chains was evaluated from the area ratio between $\nu_s(CH_2)$ and $\nu_s(CH_3)$. This ratio did not display any distinct trend indicating little change in the length of the lipid hydrocarbon chains. The peak around 3005 cm^{-1} is assigned to unsaturated ν(C–H) on –HC=CH– groups, and provides a good index for unsaturation [20]. The area of this peak reported to the area of the peak arising from $\nu_s(CH_2)$ is an established index for hydrocarbon chain unsaturation. This ratio increased as a function of the incubation time, indicating a higher concentration of unsaturated bonds in the lipid chains after ouabain treatment (Table 1). Because the polar head groups of the different lipid classes have distinct infrared features, it is possible to get information on the evolution of their relative proportions upon ouabain treatment. The relative decrease in phosphate content with respect to both the hydrocarbon chains and the ester groups (lines 3 and 4 respectively in Table 1) suggests a decrease in phospholipid content or an increase in lipids that contain no phosphate such as sphingolipids (but not sphingomyelin which contains a phosphate group), glycolipids, triglycerides or fatty acids. The peak at 1740 cm^{-1}, assigned to the ester ν(C=O) from lipids [16] and present in all lipids but sphingolipids, was not significantly decreased with respect to the hydrocarbon chain (Table 1, line 5) upon ouabain treatment. Two lipid classes have a significant contribution between 1700 and 1500 cm^{-1}: sphingolipids and phosphatidylserines as indicated by the spectra presented in Fig. 5. Difference spectra data (Fig. 5) suggest an increase in the relative concentration of PS or sphingomyelin between 24 and 36 h. Twelve hours later, the only spectrum area continuing its rise is also assigned to PS or sphingomyelin. In order to evaluate in more details the evolution of these lipids, the 179 spectra of the lipid extracts collected for different cultures and different incubation time in the presence of ouabain were fitted in the 1760–1500 cm^{-1} region

Table 1
FTIR band ratios as a function of the incubation time in the presence of 36 nM ouabain.

IR band ratio assignment	IR band ratio (%)				Evolution	Suggested interpretation
	0 h	6 h	24 h	36 h		
CH=CH/CH_2 ratio (unsaturation index)	100 (±7)	107 (±10)	126 (±7)	138 (±4)	↑	Unsaturation index ↑
CH_2/CH_3 ratio (hydrocarbon chain length)	100 (±5)	105 (±8)	101 (±7)	103 (±11)	=	Acyl chain length remains unchanged
PO_2^-/CH_2 ratio	100 (±13)	92 (±19)	63 (±6)	63 (±6)	↓	Phosphate containing lipids ↓ or fatty acids and triglycerides ↑
C=O/PO_2^- ratio (lipids without phosphate)	100 (±8)	103 (±23)	143 (±13)	147 (±14)	↑	Phosphate containing lipids ↓ or fatty acids and triglycerides ↑
C=O/CH_2 ratio (number of acyl chains)	100 (±8)	98 (±6)	90 (±5)	92 (±3)	=	Ester containing lipids =
δ(NH)/CH_2 ratio	100 (±15)	98 (±13)	132 (±10)	183 (±10)	↑	Ester containing lipids ↓ or sphingomyelin ↑

Ratios (%) were computed on cell lipid mean spectra obtained for each condition and expressed in % of the value found for non-treated cell lipids. Integration limits are: CH=CH: 3018–3002 cm^{-1}, CH_3: 2875–2868 cm^{-1}, CH_2: 2860–2842 cm^{-1}, C=O: 1762–1700 cm^{-1}, N–H: 1562–1525, and PO_2^-: 1265–1205 cm^{-1}. Data are the means of at least six cultures and are reported with the standard deviation.

by the sum of the spectrum of a PC, PS and sphingomyelin (not shown). The results of the regression indicate a clear relative decrease in PC and increase in sphingomyelin while the PS contribution remained constant. Computation of the ratio between δ_s(NH) and ν_s (CH_2) reported in Table 1 confirmed an overall increase in sphingolipids or relative decrease in ester containing lipids.

In conclusion, the data obtained on the extracted lipids strongly suggest a modification in the nature of the cell lipids and in their overall degree of unsaturation. Taken together, data presented in Table 1 and the difference spectra (Fig. 5) indicate that for the hydrocarbon chains, the length was stable but the unsaturation index strongly increased. For the polar head groups, sphingolipids relative content increased markedly as indicated by their N–H contribution but phospholipid relative content decreased upon ouabain treatment. As sphingomyelin is the most abundant sphingolipid and is a phosphate containing sphingolipid, it is likely that the relative loss of phosphate was due to the increase in other lipids that do not contain phosphate such as glycolipids, triglycerides and fatty acids.

At the present time, the plasma membrane is considered to be a dynamic entity, where specific lipid–lipid interactions occur, leading to the formation of organized structures (the so-called lipid domains) that coexist in biomembranes [33]. While the functional properties of the plasma membrane are principally dictated by proteins and their orientation within the membrane, the biophysical properties of the cell surface bilayer are imposed by lipids. Furthermore, cell signaling, lipid and protein sorting, and transport mechanisms not involving protein participation, but requiring large, local deformations of the plasma membrane (endocytosis, exocytosis, and membrane fusion events), are also determined by changes in the composition of lipids, mainly by sphingolipids (of which sphingomyelin is the most abundant) and rafts [34,35]. Many proteins involved in signal cascades require the presence of intact lipid rafts for their activation. The distinct biophysical properties of rafts lead to the hypothesis that the membrane physical state could be the cause of the activation/inhibition of cellular processes [36,37]. These evidenced that ouabain-mediated profound changes in lipid composition might be one of the major reasons why so many molecular targets are affected by cardiotonic steroids (reviewed in [8]).

Lipid composition seems also to be highly important for Na^+, K^+-ATPase activity (reviewed in [8]). In 1986, Matsuda and Iwata had already reported [38] that there is a difference in phospholipid composition of cardiac Na^+, K^+-ATPase preparations between species that are sensitive to ouabain and those that are not. Sphingomyelin is higher and phosphatidylcholine is lower in the enzymes from sensitive species than in those from insensitive ones. Furthermore, whole-genome Affymetrix microarray analysis that we performed on PC-3 cells untreated and treated with modified cardiotonic steroid UNBS1450 [39] revealed that number of enzymes involved in lipid metabolism (such as lysophospholipase-like 1, phospholipase A2-activating protein, phospholipase C, beta 1 (phosphoinositide-specific), phospholipid scramblase 1 and N-acylsphingosine amidohydrolase (non-lysosomal ceramidase) 2) are affected by the cardenolide treatment.

In future work, it would be quite interesting to investigate and compare the effect on FTIR spectra of different antitumor drugs in order to assess the potential existence of specific "molecular signature" of different classes of molecules.

While the FTIR analysis has become quite a useful tool for diagnostic purposes in oncology [7,40–45], we now suggest the use of this technology in new anti-cancer drug discovery. The present work demonstrates that a wealth of information on non-protein and non-nucleic acid molecules is available in the FTIR spectra.

Acknowledgments

R.G. is the holder of a Grant from the "Yvonne Boël" Foundation, Université Libre de Bruxelles. E.G. and R.K. are Directors of Research with the "National Fund for Scientific Research", Belgium.

The present work was supported by grants awarded by the Fonds Yvonne Boël (Brussels, Belgium), Interuniversity Attraction Poles (IAP) P6/19 (Belgium) and the Région de Bruxelles-Capitale (Brussels, Belgium). T.M. and J.D. are employees of Unibioscreen SA, Brussels, Belgium.

Appendix A. Supplementary data

Supplementary data associated with this article can be found, in the online version, at doi:10.1016/j.bbamem.2009.02.016.

References

[1] M. Suggitt, M.C. Bibby, 50 years of preclinical anticancer drug screening: empirical to target-driven approaches, Clin. Cancer Res. 11 (2005) 971–981.
[2] D. Naumann, V. Fijala, H. Labischinski, P. Giesbrecht, The rapid differentiation and identification of pathogenic bacteria using Fourier-transform infrared spectroscopic and multivariate statistical-analysis, J. Mol. Struct. 174 (1988) 165–170.
[3] D. Naumann, D. Helm, H. Labischinski, Microbiological characterizations by FT-IR spectroscopy, Nature 351 (1991) 81–82.
[4] M.A. Cohenford, B. Rigas, Cytologically normal cells from neoplastic cervical samples display extensive structural abnormalities on IR spectroscopy: implications for tumor biology, Proc. Natl. Acad. Sci. U. S. A. 95 (1998) 15327–15332.
[5] B.R. Wood, M.A. Quinn, B. Tait, M. Ashdown, T. Hislop, M. Romeo, D. McNaughton, FTIR microspectroscopic study of cell types and potential confounding variables in screening for cervical malignancies, Biospectroscopy 4 (1998) 75–91.
[6] A. Gaigneaux, C. Decaestecker, I. Camby, T. Mijatovic, R. Kiss, J.M. Ruysschaert, E. Goormaghtigh, The infrared spectrum of human glioma cells is related to their in vitro and in vivo behavior, Exp. Cell Res. 297 (2004) 294–301.
[7] R.K. Sahu, S. Mordechai, Fourier transform infrared spectroscopy in cancer detection, Future Oncol. 1 (2005) 635–647.
[8] T. Mijatovic, E. Van Quaquebeke, B. Delest, O. Debeir, F. Darro, R. Kiss, Cardiotonic steroids on the road to anti-cancer therapy, Biochim. Biophys. Acta 1776 (2007) 32–57.
[9] E. Van Quaquebeke, G. Simon, A. Andre, J. Dewelle, M. El Yazidi, F. Bruyneel, J. Tuti, O. Nacoulma, P. Guissou, C. Decaestecker, J.C. Braekman, R. Kiss, F. Darro, Identification of a novel cardenolide (2″-oxovoruscharin) from *Calotropis procera* and the hemisynthesis of novel derivatives displaying potent in vitro antitumor activities and high in vivo tolerance: structure–activity relationship analyses, J. Med. Chem. 48 (2005) 849–856.
[10] T. Mijatovic, D.B. Op, E. Van Quaquebeke, J. Dewelle, F. Darro, Y. de Launoit, R. Kiss, The cardenolide UNBS1450 is able to deactivate nuclear factor kappaB-mediated cytoprotective effects in human non-small cell lung cancer cells, Mol. Cancer Ther. 5 (2006) 391–399.
[11] O. Debeir, P. Van Ham, R. Kiss, C. Decaestecker, Tracking of migrating cells under phase-contrast video microscopy with combined mean-shift processes, IEEE Trans. Med. Imag. 24 (2005) 697–711.
[12] E. Goormaghtigh, V. Raussens, J.M. Ruysschaert, Attenuated total reflection infrared spectroscopy of proteins and lipids in biological membranes, Biochim. Biophys. Acta 1422 (1999) 105–185.
[13] E.G. Bligh, W.J. Dyer, A rapid method of total lipid extraction and purification, Can. J. Biochem. Physiol. 37 (1959) 911–917.
[14] C. Decaestecker, O. Debeir, H.P. Van, R. Kiss, Can anti-migratory drugs be screened in vitro? A review of 2D and 3D assays for the quantitative analysis of cell migration, Med. Res. Rev. 27 (2007) 149–176.
[15] J.R. Mourant, Y.R. Yamada, S. Carpenter, L.R. Dominique, J.P. Freyer, FTIR spectroscopy demonstrates biochemical differences in mammalian cell cultures at different growth stages, Biophys. J. 85 (2003) 1938–1947.
[16] H. Mantsch, M. Jackson, Molecular spectroscopy in biodiagnostics (from Hippocrates to Herschel and beyond), J. Mol. Struct. 347 (1995) 187–206.
[17] P. Lasch, M. Boese, A. Pacifico, M. Diem, FT-IR spectroscopic investigations of single cells on the subcellular level, Vib. Spectrosc. 28 (2002) 147–157.
[18] E. Benedetti, E. Bramanti, F. Papineschi, I. Rossi, E. Benedetti, Determination of the relative amount of nucleic acids and proteins in leukemic and normal lymphocytes by means of Fourier transform infrared microspectroscopy, Appl. Spectrosc. 51 (1997) 792–797.
[19] M. Diem, S. Boydston-White, L. Chiriboga, Infrared spectroscopy of cells and tissues: shining light onto a novel subject, Appl. Spectrosc. 53 (1999) 148A–161A.
[20] U.P. Fringeli, H.H. Gunthard, Infrared membrane spectroscopy, Mol. Biol. Biochem. Biophys. 31 (1981) 270–332.
[21] K.A. Oberg, J.M. Ruysschaert, E. Goormaghtigh, The optimization of protein secondary structure determination with infrared and CD spectra, Eur. J. Biochem. 271 (2004) 2937–2948.
[22] E. Goormaghtigh, J.M. Ruysschaert, V. Raussens, Evaluation of the information content in infrared spectra for protein secondary structure determination, Biophys. J. 90 (2006) 2946–2957.
[23] M. Calero, M. Gasset, Fourier transform infrared and circular dichroism spectroscopies for amyloid studies, Methods Mol. Biol. 299 (2005) 129–151.
[24] J. Nguyen, M.A. Baldwin, F.E. Cohen, S.B. Prusiner, Prion protein peptides induce alpha-helix to beta-sheet conformational transitions, Biochemistry 34 (1995) 4186–4192.
[25] C.A. Rebuffo, J. Schmitt, M. Wenning, F. von Stetten, S. Scherer, Reliable and rapid identification of *Listeria monocytogenes* and *Listeria* species by artificial neural

network-based Fourier transform infrared spectroscopy, Appl. Environ. Microbiol. 72 (2006) 994–1000.
[26] B. Rigas, S. Morgello, I.S. Goldman, P.T.T. Wong, Human colorectal cancers display abnormal Fourier-transform infrared-spectra, Proc. Natl. Acad. Sci. U. S. A. 87 (1990) 8140–8144.
[27] P.T.T. Wong, R.K. Wong, T.A. Caputo, T.A. Godwin, B. Rigas, Infrared-spectroscopy of exfoliated human cervical cells — evidence of extensive structural-changes during carcinogenesis, Proc. Natl. Acad. Sci. U. S. A. 88 (1991) 10988–10992.
[28] L. Chiriboga, P. Xie, H. Yee, V. Vigorita, D. Zarou, D. Zakim, M. Diem, Infrared spectroscopy of human tissue. I. Differentiation and maturation of epithelial cells in the human cervix, Biospectroscopy 4 (1998) 47–53.
[29] L. Chiriboga, P. Xie, V. Vigorita, D. Zarou, D. Zakim, M. Diem, Infrared spectroscopy of human tissue. II. A comparative study of spectra of biopsies of cervical squamous epithelium and of exfoliated cervical cells, Biospectroscopy 4 (1998) 55–59.
[30] B. Rigas, P.T.T. Wong, Human colon adenocarcinoma cell-lines display infrared spectroscopic features of malignant colon tissues, Cancer Res. 52 (1992) 84–88.
[31] E. Goormaghtigh, V. Cabiaux, J.M. Ruysschaert, Determination of soluble and membrane protein structure by Fourier transform infrared spectroscopy. II. Experimental aspects, side chain structure, and H/D exchange, Sub-cell. Biochem. 23 (1994) 363–403.
[32] M. Banyay, M. Sarkar, A. Graslund, A library of IR bands of nucleic acids in solution, Biophys. Chem. 104 (2003) 477–488.
[33] A. Kusumi, C. Nakada, K. Ritchie, K. Murase, K. Suzuki, H. Murakoshi, R.S. Kasai, J. Kondo, T. Fujiwara, Paradigm shift of the plasma membrane concept from the two-dimensional continuum fluid to the partitioned fluid: high-speed single-molecule tracking of membrane molecules, Annu. Rev. Biophys. Biomol. Struct. 34 (2005) 351–378.
[34] A.H. Futerman, Y.A. Hannun, The complex life of simple sphingolipids, EMBO Rep. 5 (2004) 777–782.
[35] J.C.M. Holthuis, G. van Meer, K. Huitema, Lipid microdomains, lipid translocation and the organization of intracellular membrane transport (Review), Mol. Membr. Biol. 20 (2003) 231–241.
[36] R.N. Kolesnick, F.M. Goni, A. Alonso, Compartmentalization of ceramide signaling: physical foundations and biological effects, J. Cell. Physiol. 184 (2000) 285–300.
[37] A.E. Cremesti, F.M. Goni, R. Kolesnick, Role of sphingomyelinase and ceramide in modulating rafts: do biophysical properties determine biologic outcome? FEBS Lett. 531 (2002) 47–53.
[38] T. Matsuda, H. Iwata, Phospholipid composition of cardiac (Na^+ – K^+)-ATPases from various species, Experientia 42 (1986) 405–407.
[39] T. Mijatovic, F. Lefranc, E. Van Quaquebeke, F. Van Vynckt, F. Darro, R. Kiss, UNBS1450: a new hemi-synthetic cardenolide with promising anti-cancer activity, Drug Dev. Res. 68 (2007) 164–173.
[40] A. Tfayli, O. Piot, A. Durlach, P. Bernard, M. Manfait, Discriminating nevus and melanoma on paraffin-embedded skin biopsies using FTIR microspectroscopy, Biochim. Biophys. Acta 1724 (2005) 262–269.
[41] E. Gazi, M. Baker, J. Dwyer, N.P. Lockyer, P. Gardner, J.H. Shanks, R.S. Reeve, C.A. Hart, N.W. Clarke, M.D. Brown, A correlation of FTIR spectra derived from prostate cancer biopsies with gleason grade and tumour stage, Eur. Urol. 50 (2006) 750–760.
[42] C. Krafft, L. Shapoval, S.B. Sobottka, G. Schackert, R. Salzer, Identification of primary tumors of brain metastases by infrared spectroscopic imaging and linear discriminant analysis, Technol. Cancer Res. Treat. 5 (2006) 291–298.
[43] W. Steller, J. Einenkel, L.C. Horn, U.D. Braumann, H. Binder, R. Salzer, C. Krafft, Delimitation of squamous cell cervical carcinoma using infrared microspectroscopic imaging, Anal. Bioanal. Chem. 384 (2006) 145–154.
[44] C. Krafft, S.B. Sobottka, K.D. Geiger, G. Schackert, R. Salzer, Classification of malignant gliomas by infrared spectroscopic imaging and linear discriminant analysis, Anal. Bioanal. Chem. 387 (2007) 1669–1677.
[45] T.D. Wang, G. Triadafilopoulos, J.M. Crawford, L.R. Dixon, T. Bhandari, P. Sahbaie, S. Friedland, R. Soetikno, C.H. Contag, Detection of endogenous biomolecules in Barrett's esophagus by Fourier transform infrared spectroscopy, Proc. Natl. Acad. Sci. U. S. A. 104 (2007) 15864–15869.